

THREE-STAGE SIMULATION FOR THE DEVELOPMENT OF AN ION-ACOUSTIC DOSE-DEPOSITION MAPPING SYSTEM FOR LHARA*

M. Maxouti^{†1,2,3}, H.T. Lau¹, J. McGarrigle^{1,4}, A.E. MacIntosh-LaRocque¹,
E. Harris⁵, C. Whyte⁶, J. Matheson³, J.C. Bamber⁵, B. Cox⁷, K. Long^{1,2,3}

¹ Department of Physics, Imperial College London, UK

² John Adams Institute for Accelerator Science, UK

³ Particle Physics Department, STFC Rutherford Appleton Laboratory, UK

⁴ Institut Curie-Orsay Research Center, Bat a Campus d'Orsay, France

⁵ Institute of Cancer Research and Royal Marsden NHS Foundation Trust, UK

⁶ Department of Physics, University of Strathclyde, UK

⁷ Department of Medical Physics and Biomedical Engineering, University College London, UK

Abstract

LhARA, the Laser-hybrid Accelerator for Radiobiological Applications, is proposed as a facility for the study of radiation biology using proton and ion beams. The accelerator is designed to deliver a variety of ion species over a wide range of spatial and temporal profiles at ultra-high dose rates. The variable nature of the ion yield requires that the deposited dose distribution be measured in real-time. For this purpose, an ion-acoustic dose mapping system is under development that exploits the ultrasound waves generated by the absorption of the ion beam energy. A three-stage simulation has been developed to evaluate the feasibility of this approach. For the preliminary demonstration of simulation functionality for dose-map reconstruction, a hemispherical sensor array was specified to evaluate the recovery of the relative spatial distribution of the absorbed dose using an iterative time-reversal algorithm.

INTRODUCTION

Ion beam therapy (IBT) is a clinical therapy that uses ionising radiation such as protons and other light ions to treat tumours by preventing or killing malignant cells that proliferate [1]. Ions provide an advantageous dose distribution, relative to x-rays, due to the deposition of the maximum dose in the "Bragg peak", at the end of their range. This property is favourable as it enables selective treatment while sparing the healthy cells around the tumour, and therefore, the accurate localization of the Bragg peak is extremely important.

An on-the-fly, non-invasive system is proposed that can provide a quantitative 4D dose deposition profile and Bragg peak localization for pre-clinical research and, at a later stage, provide clinical measures of the deposited energy distribution in tissue. The system proposed will minimize delivery uncertainties, enable a more reliable, real-time pulse-

to-pulse adaptive treatment plan, as well as enable hypofractionation to be achieved more accurately (delivery of fewer, more intense doses) [2].

The development of the proposed system for LhARA [3] relies on ion-acoustic imaging, which is based on ultrasound waves emitted as a result of the transient pressure rise when the beam energy is absorbed and causes a rise in temperature [4]. Due to the short pulses (10—40 ns) delivered by LhARA, the pressure increase generated by the almost instantaneous energy deposition satisfies the stress confinement criterion necessary for the efficient generation of acoustic (pressure) waves [5]. Although limited to parts of the body that are not obstructed by intervening bone or gas, the ion-acoustics approach has several advantages including good spatial resolution, large penetration depth and *in-vivo* applicability. In addition, conventional ultrasound images can be used to co-register information about blood flow and tissue motion with the dose maps and anatomy.

METHOD

To confirm the fundamental ability of ion-acoustic imaging to provide the beam deposition profile, a three-stage simulation has been developed using Geant4 [6] and k-Wave [7]. The three stages include the generation of the beam-induced energy distribution, the pressure wave generation, propagation and detection, and the pressure-map reconstruction. To compute each stage of the simulation, the active volume was split into cubic voxels with sides 0.1 mm.

A water phantom was modelled in Geant4 and irradiated with proton beams with energies up to 70 MeV. The energy deposited by the beam was calculated as a function of position and time. The time-dependent 3D energy distribution was then used as the source in k-Wave to simulate the generation of acoustic waves and their propagation in three-dimensional space. A hemispherical acoustic sensor array was also simulated so that the reconstruction of the pressure distribution using an iterative time-reversal algorithm could be evaluated [8].

* This work is supported by the Science and Technology Facilities Council (STFC).

† m.maxouti21@imperial.ac.uk

ABSORBED ENERGY DISTRIBUTION

Water phantom A schematic diagram of the water phantom, that acts as the propagating medium, is shown in Figure 1. The beam enters through a 50 μm thick kapton foil at the end of a 15 mm diameter tube. This ensures that the Bragg peak of a 20 MeV proton beam occurs at the centre of the phantom. The energy deposited by the beam were recorded for use in the second stage of the simulation.

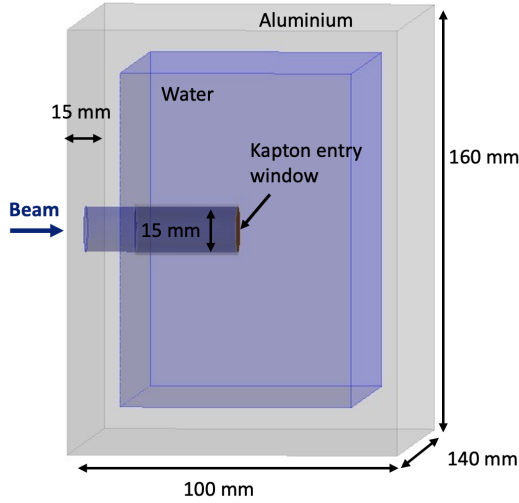


Figure 1: Geant4 simulation of the water phantom to be used as the propagating medium in the ionacoustics proof-of-principle simulation.

PRESSURE WAVE GENERATION, PROPAGATION & DETECTION

Pressure waves The pressure wave generation and evolution inside the phantom was simulated in k-Wave. The source pressure distribution at location \mathbf{r} and temperature T , $p_0(\mathbf{r}, T)$, was calculated from the energy depositions given by Geant4, $E(\mathbf{r}, T)$, using Equation 1 [9], where Γ is the dimensionless Grüneisen coefficient and $\rho(\mathbf{r}, T)$ is the target mass density.

$$p_0(\mathbf{r}, T) = \Gamma(\mathbf{r}, T) \times E(\mathbf{r}, T) \times \rho(\mathbf{r}, T) \quad (1)$$

The Grüneisen coefficient is a measure of the efficiency of converting the absorbed heat energy to induced pressure and is calculated using Equation 2 [9], where c is the speed of sound in the medium, β the thermal expansion coefficient and C_p the specific heat capacity.

$$\Gamma(\mathbf{r}, T) = \frac{c^2 \beta}{C_p} \quad (2)$$

For water at room temperature, the Grüneisen coefficient is approximately 0.11 [10] and this value has been used for the simulation. In addition, perfectly matched layer boundaries have been implemented in the simulation to prevent waves from being reflected.

The resulting source pressure distribution of a 20 MeV proton beam in the three orthogonal planes is shown in Figure 2.

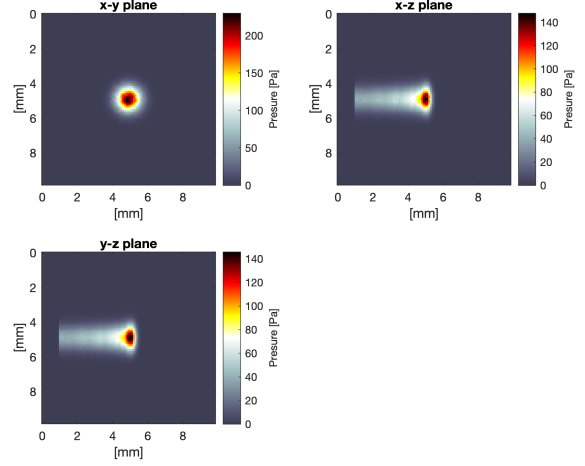


Figure 2: Source pressure distribution, in the three orthogonal planes, caused by the energy depositions of a 20 MeV proton beam consisting of 100000 particles. The beam had a 2 mm radius, 35 ns pulse duration and 2% energy spread. Voxel size: 0.1 mm.

Acoustic sensor A hemispherical-shaped sensor array that would allow the collection of spatially sampled pressure data was simulated in k-Wave. The hemispherical shape was chosen because it provides good lateral resolution due to its large spatial and angular coverage. The sensor array, shown in Figure 3, has an 8 mm diameter with 300 disc elements, each with a 0.2 mm diameter, placed evenly on its surface. The center of curvature of the hemisphere was placed at a proton beam axial distance of 2.5 mm from the entrance window, to allow the field of view to include the Bragg peak as well as some of the upstream distribution.

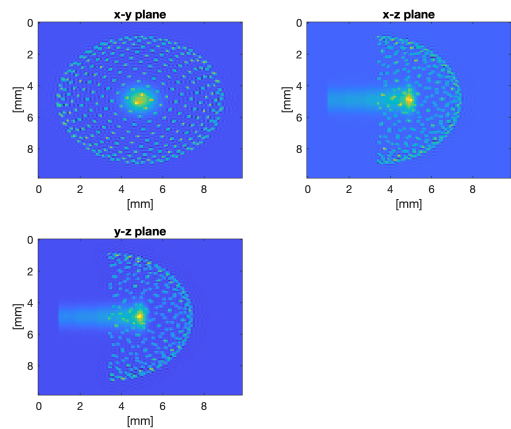


Figure 3: Acoustic sensor array geometry and location relative to the proton beam energy depositions caused by a 20 MeV proton beam in the water phantom. Voxel size: 0.1 mm.

PRESSURE-MAP RECONSTRUCTION

The pressure data collected by the sensor array were used to reconstruct the 3D pressure distribution caused by the transient energy deposition of the beam using a time-reversal reconstruction algorithm.

The time-varying pressure signals detected at each element were propagated backwards in time, each element being treated as a point source. During backpropagation, the time-reversed waves interfere to form the reconstructed image of the pressure distribution.

The time-reversal reconstruction was iterated to obtain an improved estimate of the pressure distribution. To do this, the reconstructed time-series was subtracted from the original time-series to calculate a residual. This residual was used to form another image that was then added to the previous image to give an improved estimate. Six iterations were regarded as sufficient for the reconstruction to converge.

RESULTS & DISCUSSION

The temporal pressure distribution received by the acoustic sensor array is shown in Figure 4. The sudden pressure increase is explained by the energy depositions of the beam that cause an increase in temperature and pressure, and the subsequent sudden fall is explained by the release of the pressure waves. Subsequent peaks correspond to reflections off the kapton-air boundary.

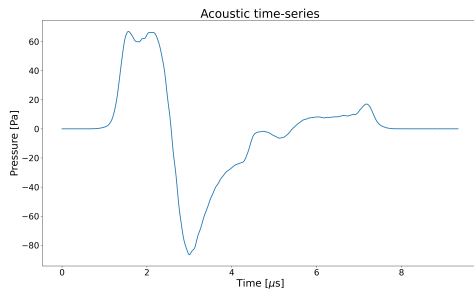


Figure 4: Temporal pressure distribution from the summed element data received by the acoustic sensor array.

The results of the reconstruction after six iterations of the time-reversal algorithm are shown in Figures 5 and 6. Figure 5 shows the reconstructed source pressure distribution in the three orthogonal planes which compares well with the true source pressure distribution in Figure 2.

Figure 6 provides the z-axis 1D profile through the reconstructed source pressure distribution. From this graph, it is clear that an increase in the number of iterations used in the reconstruction algorithm results in a more accurate pressure reconstruction.

Both Figures 5 and 6 show a clear Bragg peak as expected. The departures of the reconstructed source pressure from the true source pressures at axial distances around the Bragg peak can be explained by limitations in the sampling frequency of the simulation or the sensor elements in the acoustic array being too far apart.

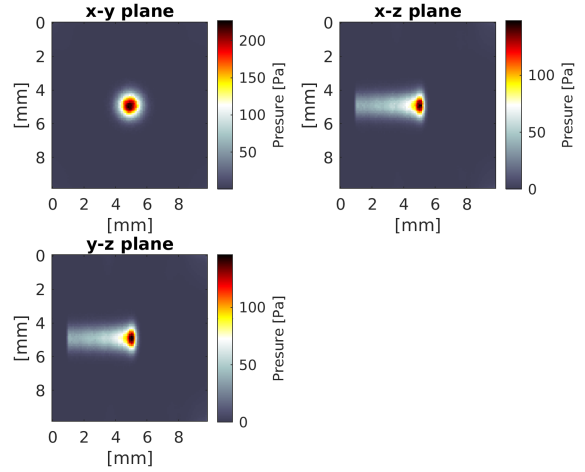


Figure 5: Reconstructed pressure distribution in the three orthogonal planes, using the data received by the acoustic sensor array and an iterative time-reversal reconstruction algorithm. Voxel size: 0.1 mm.

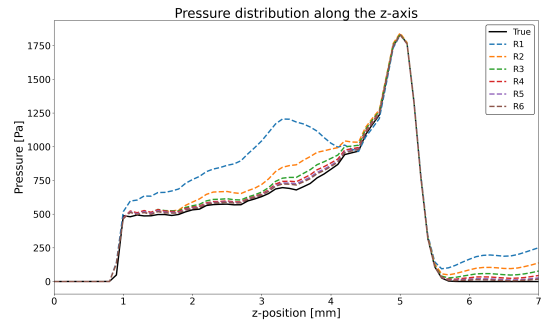


Figure 6: Reconstructed source pressure along the axis of beam propagation using 6 iterations of the time-reversal algorithm. Voxel size: 0.1 mm. True: source pressure caused by the energy depositions of the proton beam in the water phantom. R1-6: estimated source pressure, where the number corresponds to the total number of iterations used in the reconstruction algorithm.

CONCLUSION

The iterative time-reversal algorithm gives an accurate reconstruction of the 3D pressure distribution using the pressure data received by the simulated acoustic sensor array. Increasing the number of iterations used in the reconstruction algorithm improved the estimate of the source pressure distribution, and after six iterations, sub-millimeter accuracy has been achieved.

Future simulations can take into account realistic transducer responses and be used to evaluate signal-to-noise ratio requirements. Finally, when validated, the simulation can be used to optimize the sensor array design.

In conclusion, this paper reports the proof-of-principle development of a simulation that can lead to a system that would enable online 3D dosimetry during ion-beam therapy with the LhARA accelerator.

REFERENCES

- [1] Lehrer EJ, Prabhu AV, Sindhu KK, Lazarev S, Ruiz-Garcia H, Peterson JL, Beltran C, Furutani K, Schlesinger D, Sheehan JP, Trifiletti DM. Proton and Heavy Particle Intracranial Radiosurgery. *Biomedicines*. 2021 Jan 3;9(1):31. doi: 10.3390/biomedicines9010031. PMID: 33401613; PMCID: PMC7823941
- [2] Hypofractionated Radiotherapy - an overview, *ScienceDirect Topics*, <https://www.sciencedirect.com/topics/medicine-and-dentistry/hypofractionated-radiotherapy>
- [3] LhARA : The Laser-hybrid Accelerator for Radiobiological Applications. *Frontiers in Physics, Medical Physics and Imaging*, 8. 567738, <https://doi.org/10.3389/fphy.2020.567738>
- [4] Haffa, D., Yang, R., Bin, J. et al. I-BEAT: Ultrasonic method for online measurement of the energy distribution of a single ion bunch. *Sci Rep* 9, 6714 (2019), <https://doi.org/10.1038/s41598-019-42920-5>
- [5] Eshel Faraggi, Shijun Wang, and Bernard Gerstman "Stress confinement, shock wave formation, and laser-induced damage", *Proc. SPIE 5695, Optical Interactions with Tissue and Cells XVI*, (15 April 2005) <https://doi.org/10.1117/12.589469>
- [6] CERN. 2020. User Documentation, https://geant4.web.cern.ch/support/user_documentation
- [7] www.k-wave.org. (n.d.). k-Wave: A MATLAB toolbox for the time domain simulation of acoustic wave fields, <http://www.k-wave.org>
- [8] Otero, J.; Felis, I.; Herrero, A.; Merchán, J.A.; Ardid, M. Bragg Peak Localization with Piezoelectric Sensors for Proton Therapy Treatment. *Sensors* 2020, 20, 2987, <https://doi.org/10.3390/s20102987>
- [9] Freijo C, Herraiz JL, Sanchez-Parcerisa D, Udias JM. Dictionary-based protoacoustic dose map imaging for proton range verification. *Photoacoustics*. 2021 Jan 16;21:100240. doi: 10.1016/j.pacs.2021.100240. PMID: 33520652; PMCID: PMC7820918,
- [10] Jones KC, Nie W, Chu JCH, et al. Acoustic-based proton range verification in heterogeneous tissue: simulation studies. *Phys Med Biol*. 2018;63(2):025018, doi:10.1088/1361-6560/aa9d16